Study on stress sensitivity of bedding fractures and sand-filled fractures in shale oil reservoirs

Haojia Li[1], Chenwei Liu[1,*], Silin Yan[1] and Sen Lv[1]

[1]School of Petroleum Engineering in China University of Petroleum (East China), Qingdao, 266580, China

Abstract. Shale oil reservoirs are characterized by low porosity and ultra-low permeability, and hydraulic fracturing technology is needed to realize industrial oil flow. The sand-filled fractures formed in the shale fracturing process and the bedding fractures developed in the reservoir itself interact to form a shale oil fracture network system, which is the main migration channel for shale oil production. Studies have shown that the higher the degree of fracture development, the stronger the stress sensitivity of the reservoir, and the stress sensitive damage is an important factor that causes the decline of reservoir seepage capacity during shale oil production. In this paper, based on the shale samples in the Jiyang Depression, the flow capacity experiments of bedding fractures and sand-filled fractures were carried out to analyze the stress sensitivity characteristics of shale bedding fractures and sand-filled fractures, and to clarify the seepage capacity decline mechanism of complex fractures in shale. Provide experimental data and theoretical support for productivity prediction of block shale reservoirs after fracturing.

1 Introduction

The permeability of shale reservoirs is extremely low [1]. In laboratory experiments, the gas pressure pulse attenuation method [2] is generally used to obtain the permeability. However, for shale oil reservoirs, the actual flow medium is liquid phase, and the gas permeability results often cannot accurately characterize shale. The real flow characteristics of the oil reservoir, so this section uses the hydraulic pressure pulse method to measure the permeability of the core. On this basis, based on the constant confining pressure, the stress sensitivity of the reservoir is discussed through the change of reservoir permeability under different flow pressure conditions. The hydraulic pressure pulse technology is used to obtain the core permeability under different effective stresses [3], so as to reveal the effect mechanism of effective stress on the core permeability of bedding fractures.

Testing the conductivity of sand-filled fractures is crucial to the design of fracturing operations [4]. Common conductivity tests can be divided into two types [5]: sandstone-filled slab test and sand-filled core test. Since the slab test cannot impose confining pressure, this chapter chooses to take core rock samples and prepare shale cores containing sand-filled fractures through a Brazilian splitting device, and simulate the elastic development process to determine the confining pressure and reduce the flow pressure. Carry out relevant stress-sensitive characteristic tests and explore the influence of relevant factors.

2 Stress sensitivity experiment of shale with bedding fractures

2.1 Experimental principle

The pressure pulse method is used to test the permeability of shale cores [6]. A standard chamber with equal volume is set at both ends of the core holder. By giving an instantaneous pressure difference change to the standard chambers at both ends of the core holder, the non-Darcy seepage equation and the continuous Equation to calculate the permeability of the core.

$$ln\frac{\Delta p(t)}{\Delta p(0)} = ln\,B - \left[\frac{KA}{\mu L}\left(\frac{1}{S_1}+\frac{1}{S_2}\right)\right]t \tag{1}$$

In the formula, p is the flow pressure; L, A, K are the core length, core cross-sectional area, and permeability, respectively; μ is the fluid viscosity; t is the time; S_1 and S_2 are the compression storage volumes of the upstream and downstream standard chambers, respectively.

2.2 Experimental equipment and experimental materials

The equipment used in the pressure pulse method experiment mainly includes a core holder, a pressure data acquisition and processing system, and a pressure pulse system. The flow chart of the experimental device is shown in Figure 1.

* Corresponding author: 20170018@upc.edu.cn

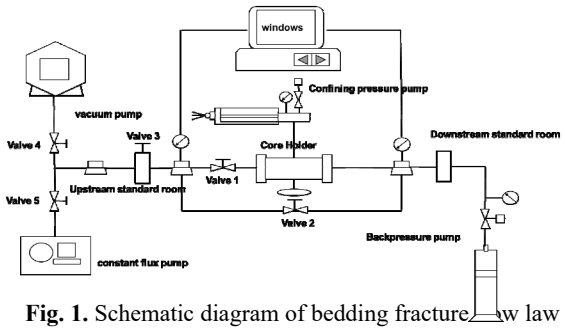

Fig. 1. Schematic diagram of bedding fracture flow law experiment

The kerosene and cores used in the experiment were actually cored rock samples from Shengli Oilfield. According to the fracture development of the cores, the cores were divided into two types: those with bedding fractures and those without bedding fractures (matrix type). The specific parameters of the cores are shown in Table 1 [7].

Table 1. Shale Core Parameters

Serial number	length/mm	diameter/mm	Development status of bedding fractures
1#	25.5	27.7	underdeveloped
2#	25.2	24.9	underdeveloped
3#	26.1	24.6	development
4#	24.7	24.7	development
5#	25.5	25.1	development
6#	25.6	24.8	development

Figure 2 is the core used in the experiment.

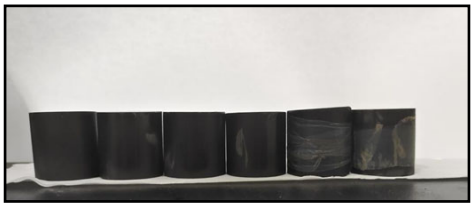

Fig. 2. The physical map of the core required for the experiment

2.3 Experimental procedure

① Put the core into the core holder, and after the water-filled confining pressure pump is exhausted, use the pressure tracking mode to gradually pressurize the test system.

② The confining pressure is gradually increased from 0 to 5MPa, and then the pressure difference between the confining pressure and the flow pressure is always kept at 5MPa. Ensure that the permeability of bedding fractures will not be significantly damaged in advance, and can also avoid damage to the holder sleeve.

③ Fix the flow pressure at 25MPa, and continue to increase the confining pressure until it reaches 50MPa. Let it stand for a certain period of time to allow the pressure to spread evenly in the core.

④ Start to record the upstream and downstream fluid pressure data, rotate the needle valve, pressurize the upstream fluid of the core, and generate a pulse of 0.4~0.8MPa, and stop recording the data after the upstream and downstream pressures reach balance.

⑤ Keep the confining pressure constant, reduce the fluid pressure to 20MPa, and repeat the experimental operation of step ④.

⑥ Keep the confining pressure constant, continue to reduce the fluid pressure to 15MPa, 10MPa, 5MPa and repeat the experimental operation of step ④.

⑦ Process the upstream and downstream pressure data to obtain the permeability of the core under various flow pressure states.

2.4 Experimental results and analysis

Taking the data of No. 1# core, flowing pressure 25MPa, and confining pressure 50MPa as an example, the experimental data processing is carried out.

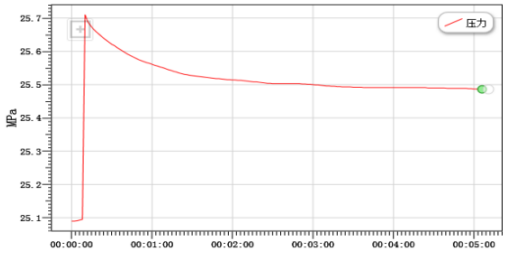

Fig. 3. Core upstream pressure data curve

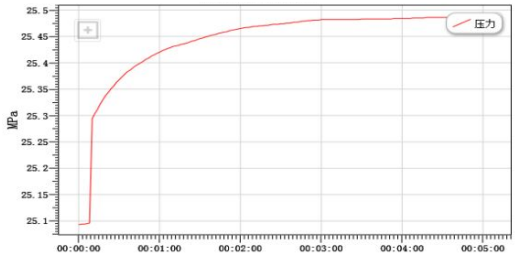

Fig. 4. Core downstream pressure data curve

Fig. 3 is the pressure variation curve of the upstream end with time, and Fig. 4 is the pressure variation curve of the downstream end of the rock core. As shown in the figure, the pressure at the upstream end gradually decreases and stabilizes with time, while the pressure at the downstream end is the opposite, increasing first and then gradually stabilizing. Make the difference between the upstream and downstream pressure values to obtain the upstream and downstream pressure difference, substitute it in to find out, and draw the curve shown in Figure 5, and perform fitting.

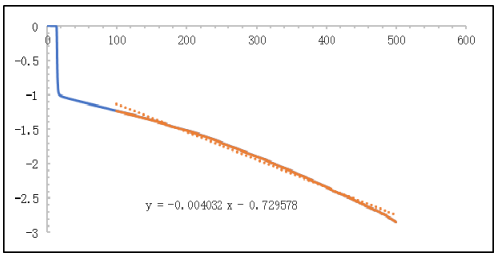

Fig. 5. Logarithmic fitting graph of core data

According to the formula $\ln\frac{\Delta p(t)}{\Delta p(0)} = A_0 + A_1 t$

The slope of the straight line is A_1。

$$A_1 = \frac{KA}{\mu L}\left(\frac{1}{S_1}+\frac{1}{S_2}\right) \tag{2}$$

Substitute A = 4.79 cm^2, L = 2.55 cm, μ = 2.355 mPa·s, S_1 = 0.014876 cm^3, S_2 = 0.003415 cm^3, derive the permeability K = 0.001392mD.

Calculate the permeability of other points in the same way, and normalize [8] the obtained core permeability data to obtain Table 2.

Table 2. Core normalized permeability

Effective stress/MPa	Normalized permeability					
	1#	2#	3#	4#	5#	6#
25	1.00	1.00	1.00	1.00	1.00	1.00
30	0.85	0.91	0.16	0.18	0.85	0.87
35	0.67	0.73	0.07	0.08	0.69	0.55
40	0.56	0.67	0.03	0.04	0.46	0.49
45	0.39	0.57	0.02	0.03	0.30	0.29

The above comparison shows that the stress sensitivity of the permeability of 1# and 2# matrix cores is weak, while the stress sensitivity of the 3# and 4# two bedding fracture cores with inflection points is the strongest, while the 5# and 6# cores have the strongest stress sensitivity characteristics. The stress-sensitivity characteristic of is between the two, and is closer to matrix-type cores. The possible reason is that although cracks are observed on the surface of 5# and 6#, the cracks may not penetrate the entire core, so the stress sensitivity characteristics are closer to matrix cores.

3 Stress Sensitivity Experiment of Shale Containing Sand Filled Fractures

3.1 Experimental principle

The experimental principle can be derived from Darcy's law (see formula 3), and the core fracture data can be converted to Darcy's formula to obtain formula 4 for calculating fracture conductivity [9]:

$$Q = \frac{kA\Delta p}{\mu L} \tag{3}$$

$$C_f = kw_f = \frac{Q\mu}{\Delta p}\cdot\frac{L}{d} \tag{4}$$

where: C_f is the conductivity of sand-filled fractures; k is the permeability of sand-filled fractures; w_f is the fracture width; μ is the fluid viscosity under experimental conditions; Q is the liquid flow rate; L is the length of the major axis of the core; d is the diameter of the core; $\triangle p$ is the pressure difference.

3.2 Experimental device and experimental materials

The experimental device is the same as the bedding fracture flow law experiment. The core is selected from actual coring in Shengli Oilfield, the fluid is kerosene, and the required proppant is 40/70 mesh, 70/120 mesh and 100/140 mesh quartz sand. (Fig. 6. And Fig. 7.)

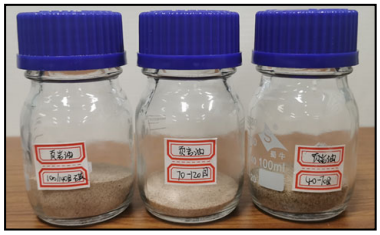

Fig. 6. Proppant particles needed for experiment

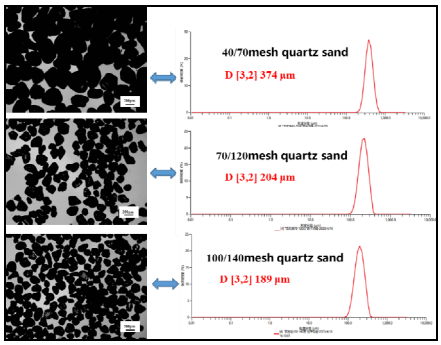

Fig. 7. Proppant scanned by particle size analyzer

3.3 Sand-filled fracture core preparation

Artificial fractures are the main flow channels for shale reservoir fluids, and their stress sensitivity is closely related to the concentration of proppant in fractures. Due to the well-developed shale bedding and high brittleness, if the force direction is not aligned with the bedding fractures during artificial fractures, stress dislocation is prone to occur, resulting in a low success rate of fractures. The conventional wire-cutting method of fracture creation is too smooth and flat, which is quite different from the fracture surface characteristics of field pressure fractures.

For this purpose, artificial seams are created using the Brazilian split method [10], in which a circular specimen is subjected to pressure between two symmetrical pressure loading points. This pressure loading will cause the sample to generate tensile stress around the loading point, and eventually lead to the

formation of a crack in the center of the sample. The diagram of the experimental setup is shown in Figure 8.

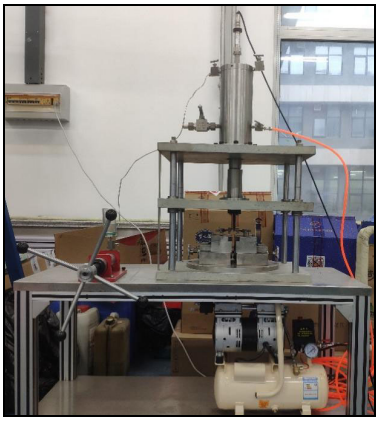

Fig. 8. Brazil splitting device

After the fracturing is completed, because the surface of the sample is rough and uneven, the core sample needs to be polished for subsequent observation, testing or analysis. When performing core grinding, a micro lathe (as shown in Figure 9) is commonly used to gradually remove the unevenness and roughness of the sample surface to obtain a smoother sample surface. It should be noted that when performing core grinding, care should be taken to avoid additional damage to the sample. In addition, care should be taken to keep the sample wet during the grinding process to avoid thermal damage and dry cracking of the sample surface.

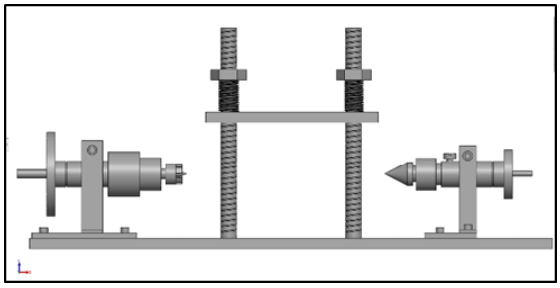

Fig. 9. Core grinding device

3.4 Experimental results and analysis

3.4.1 Influence of different sand concentration on the flow conductivity of sand-filled fractured core

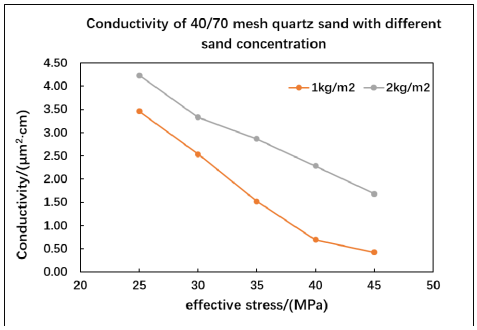

Fig. 10. 40/70 mesh conductivity

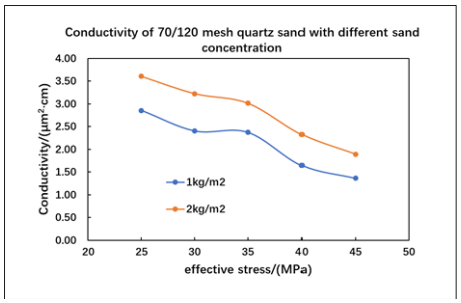

Fig. 11. 70/120 mesh conductivity

According to Figure 10 and Figure 11, the same type of proppant can be obtained, the higher the sand concentration, the stronger the conductivity [11]. This is because the sanding concentration determines the width of the cracks after the proppant is laid. The higher the sanding concentration is, the greater the impact on the mutual support between the particles laid in multiple layers (when the layers are stacked, the particles in the upper and lower layers form more contact points, Distributed pressure), the less likely the particles are broken, the greater the conductivity.

3.4.2 Effects of different proppant particle sizes on the conductivity of sand-filled fractured core

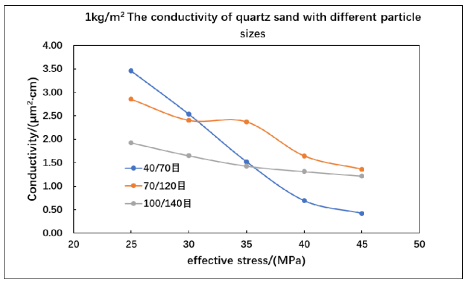

Fig. 12. 1kg/m^2 sand concentration different proppant particle size

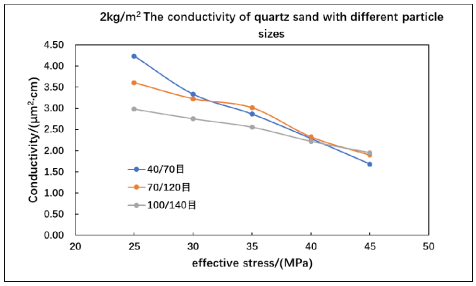

Fig. 13. 2kg/m^2 sand concentration different proppant particle size

From Fig. 12 and Fig. 13, it can be seen that the larger the proppant particle size, the lower the crushing strength, and the larger the pores formed in the fracture due to dense accumulation, the more likely to be broken when subjected to the closing pressure, and the fracture width changes more obviously [12]. The denser oil flow channel reduces the flow conductivity. The proppant particles with large particle size have greater initial conductivity, but compared with particles with small

particle size, the flow conductivity decreases with the increase of closure pressure.

4 Conclusion

(1) Based on the one-dimensional unsteady-state seepage equation, the experimental method of pressure pulse liquid measurement of permeability is constructed, which has the advantages of high precision and short test time; simulates the elastic development process, and uses the test method of constant confining pressure and variable flow pressure to target The stress sensitivity test experiments of matrix-type and bedding-fractured cores show that: with the increase of effective stress, the permeability of matrix-type and bedding-fractured cores show a decreasing trend, and the cores with more bedding fractures show a stronger stress sensitivity. characteristics, and the closure pressure of fractures is about 30 MPa; in contrast, the stress sensitivity of matrix cores is weak, and the permeability basically decreases linearly with the increase of effective stress.

(2) On the basis of improving the core preparation of sand-filled fractures, the test experiment of fracture conductivity with constant confining pressure and variable flow pressure was carried out. The results show that large particle size and high sand-fill concentration will form higher fracture conductivity Capability; large particle size proppants have strong stress-sensitivity in filling fractures, and increasing the sand-fill concentration can effectively reduce the stress-sensitivity of sand-filling fractures.

References

1. Gao Q, Liu J, Leong Y K, et al. A Review of Swelling Effect on Shale Permeability: Assessments and Perspectives[J]. Energy & Fuels, 2023, 37(5): 3488-3500.
2. Zhao Y, Zhang K, Wang C, et al. A large pressure pulse decay method to simultaneously measure permeability and compressibility of tight rocks[J]. Journal of Natural Gas Science and Engineering, 2022, 98: 104395.
3. Shao J, You L, Jia N, et al. Salt crystal: Natural proppant for enhancing shale reservoir production[J]. Energy, 2023, 262: 125569.
4. Tao Z, Liu C, He Q, et al. Detection and treatment of organic matters in hydraulic fracturing wastewater from shale gas extraction: A critical review[J]. Science of The Total Environment, 2022, 824: 153887.
5. Zhu L, Ma Y, Cai J, et al. Key factors of marine shale conductivity in southern China—Part II: The influence of pore system and the development direction of shale gas saturation models[J]. Journal of Petroleum Science and Engineering, 2022, 209: 109516.
6. Bai J, Kang Y, Chen M, et al. Investigation of multi-gas transport behavior in shales via a pressure pulse method[J]. Chemical Engineering Journal, 2019, 360: 1667-1677.
7. Gale J F W, Laubach S E, Olson J E, et al. Natural fractures in shale: A review and new observations[J]. AAPG bulletin, 2014, 98(11): 2165-2216.
8. Xu J, Bu Z, Li H, et al. Permeability models of hydrate-bearing sediments: A comprehensive review with focus on normalized permeability[J]. Energies, 2022, 15(13): 4524.
9. Ghanizadeh A, Bhowmik S, Haeri-Ardakani O, et al. A comparison of shale permeability coefficients derived using multiple non-steady-state measurement techniques: Examples from the Duvernay Formation, Alberta (Canada)[J]. Fuel, 2015, 140: 371-387.
10. Hou B, Zeng Y, Fan M, et al. Brittleness evaluation of shale based on the brazilian splitting test[J]. Geofluids, 2018, 2018.
11. Zheng X, Chen M, Hou B, et al. Effect of proppant distribution pattern on fracture conductivity and permeability in channel fracturing[J]. Journal of Petroleum Science and Engineering, 2017, 149: 98-106.
12. Huang J, Hao Y, Settgast R R, et al. Validation and application of a three-dimensional model for simulating proppant transport and fracture conductivity[J]. Rock Mechanics and Rock Engineering, 2022: 1-23.